

**LITHIUM AND LITHIUM ISOTOPES IN TOURMALINE AS
INDICATORS OF CRYSTALLIZATION PROCESSES: A STUDY OF
SAN DIEGO COUNTY PEGMATITES, CALIFORNIA**

A Thesis
presented to
the Faculty of the Graduate School
at the University of Missouri-Columbia

In Partial Fulfillment
of the Requirements for the Degree

Master of Science

by
JENNIFER MALONEY

Dr. Peter Nabelek, Thesis Advisor

May 2007

The undersigned, appointed by the dean of the Graduate School, have examined the thesis entitled

LITHIUM AND LITHIUM ISOTOPES IN TOURMALINE AS INDICATORS OF
CRYSTALLIZATION PROCESSES: A STUDY OF SAN DIEGO COUNTY
PEGMATITES, CALIFORNIA.

presented by Jennifer Maloney,

a candidate for the degree of Master of Science,

and hereby certify that, in their opinion, it is worthy of acceptance.

Dr. Peter Nabelek

Dr. Alan Whittington

Dr. Michael Glascock

ACKNOWLEDGEMENTS

This work could not have been completed without the help and support of many individuals, whom I would like to acknowledge here. First of all, I would like to acknowledge my advisor Peter Nabelek, who was always available to give guidance and insight, and gave me the opportunity to see parts of the country that were, perhaps, hotter than the surface of the sun, but also some of the most beautiful places I've ever seen. Thank you for having such a comfortable chair in your office. Also, my committee members, Alan Whittington, who provided many interesting and stimulating conversations, many of which were in his "second office", and Michael Glascock. Funding for all my adventures for this project was provided by the National Science Foundation. I would also like to give Mona Sirbescu and Jim Student from Central Michigan University a heartfelt thank you for teaching me in the field and being so helpful with all my questions. An extra thank you goes to Mona for fluid inclusion data and copies of field notes. I would like to acknowledge our guides in San Diego County, Matt Taylor and Jeff Patterson, for showing us all of the mines and their passionate discussions about pegmatite development, and the mine owners, Dana Gochenour, Louis Spaulding Jr., and Bill Larson for allowing us to sample while they were working hard.

Thank you to Carol Nabelek for all your help running the samples on the ICP-OES. Li isotope analyses were done at the Geochemistry Laboratory at the University of Maryland-College Park. I would personally like to thank Ralf Halama for all his guidance and patience when teaching me how to run samples through the columns and for analyzing the samples.

I graciously acknowledge the faculty of the Geological Sciences Department of Mizzou, whose classes fed my interest and love of geology. The completion of this work would never have been possible without the support and friendship of my fellow grad students, especially Angie, Scott, Carolina, and Geoffroy, who were always there to pick me up when I fell, and were always willing to go for a coffee run. Thank you to Mike Wise for introducing me to and feeding my passion for pegmatites. Also to Lindsay, your support and friendship over the years is what has grounded me and reminded me of what is important in life. Above all, I would also like to thank my family, especially Mom and Dad, for being so supportive, encouraging, and loving. You are my rock, without you, I could not have accomplished any of this. Lastly, thank you to Brian, even though you are so far away, your support and encouragement means more to me than I could ever express in words. Thank you for being there and for everything that you do.

TABLE OF CONTENTS

	Page
Acknowledgements _____	ii
Abstract _____	vii
Introduction _____	1
Background Geology _____	4
<i>San Diego Pegmatite Field</i> _____	8
<i>Cryo-Genie</i> _____	10
<i>Little Three</i> _____	10
<i>San Diego Mine</i> _____	12
Methods _____	13
<i>Bulk Li Concentrations</i> _____	13
<i>Li Isotope Ratios</i> _____	14
Results _____	17
<i>Cryo-Genie</i> _____	18
<i>Little Three</i> _____	22
<i>San Diego Mine</i> _____	25
Discussion _____	28
<i>Lithium Concentration and the Crystallization Process</i> _____	28
<i>Initial Lithium Concentration of the Melt</i> _____	30
<i>Lithium Isotopic Fractionation</i> _____	35
Conclusions _____	42
References _____	44

LIST OF FIGURES

Figure	Page
1. Map of North American Mesozoic Batholiths and Peninsular Ranges Batholith ____	5
2. Map of San Diego County, California _____	9
3. Plot of $\delta^7\text{Li}$ vs. ppm Li for All Samples _____	18
4. Sketch of the Green Ledge at the Cryo-Genie Mine _____	19
5. Sketch of the Pay Day Pocket at the Cryo-Genie Mine _____	21
6. Sketch of the Topaz Ledge at the Little Three Mine _____	24
7. Li Concentration of Tourmaline in Different Zones _____	26
8. $\delta^7\text{Li}$ Ratio of Tourmaline in Different Zones _____	27
9. Tourmaline Crystal Structure _____	38
10. Schematic of Li and Li Isotopic Behavior in a Pegmatitic Melt _____	41

LIST OF TABLES

Table	Page
1. Lithium concentration and isotopic composition of tourmaline _____	17
2. Mass balance data for $C_0(\text{Li})$ of pegmatitic melt _____	34
3. Tourmaline granite composition from Black Hills, South Dakota _____	35

ABSTRACT

The pegmatites of San Diego County, California, are part of the Mesozoic Peninsular Ranges Batholith of southwestern California and Baja California, Mexico. In these lithium-cesium-tantalum (LCT) type pegmatites, tourmaline is the main reservoir for Li. Due to the incompatibility of Li in most granitic melts and tourmaline's ability to incorporate large concentrations of Li, the concentration of Li in the tourmaline can serve as a petrogenic indicator for pegmatite crystallization processes. Three pegmatites were studied, Cryo-Genie, Little Three, and San Diego. Their footwalls are characterized by line rock, a rhythmically layered aplite with oscillating changes in mineralogy from quartz plus albite-rich bands to tourmaline-rich bands. Above the line rock is the pegmatite zone, characterized by large euhedral Na-feldspar near the footwall and K-feldspar near the hanging wall, quartz, and tourmaline, commonly as graphic intergrowths towards the central pocket zone. Large euhedral, and sometimes gem and specimen-quality crystals, are found in the miarolitic cavities of the pocket zone.

The Li concentrations in corresponding textural zones are similar in all three pegmatites. Tourmaline from the line rock has the lowest Li concentrations, 56-70 ppm. Li concentrations in the pegmatitic zone are significantly larger, 22-517 ppm, with the most Li occurring in the pockets (265-5075 ppm in tourmaline and ~9100 ppm in fluid inclusions). The enrichment in incompatible Li from the wall zones towards the pocket indicates that the dikes crystallized inward from the wall rock contact. The line rock appears to have crystallized until the melt reached fluid saturation, at which point, fluid

and melt separated to form the pegmatite and the pockets, respectively. Li was strongly partitioned in favor of the fluid.

The initial concentration of Li in the melt was estimated by mass-balance to have been ~1120 ppm, which is significantly higher than in leucogranites that are related to LCT pegmatite fields (10's to 100's ppm Li). The elevated amounts of Li and H₂O that occur in pegmatitic dikes lower the melt viscosity, and therefore increase the diffusivity of elements through the melt by depolymerizing the SiO₄ tetrahedra network. The large crystal size and low crystallization temperatures (<500° C) suggest that these pegmatitic dikes crystallized from a highly-fluxed, low viscosity melt through a process similar to that described by Jahns and Burnham (1969).

The isotopic composition of tourmaline is reflective of the medium from which it crystallized and is controlled by the coordination of Li in that medium. ⁷Li prefers sites with smaller coordination numbers and stronger bonds while ⁶Li fractionates into weaker sites with higher coordination numbers. Li is tetrahedrally coordinated in the melt as Li₂Si₂O₅ or Li₂SiO₃, octahedrally coordinated in tourmaline, and as the hydrated ion [Li(H₂O)₄]⁺ in the fluid (Wunder *et al.*, 2007). Tourmaline in the line rock has δ⁷Li +12.3 to +15.1 and would have crystallized from a melt that was isotopically heavier as ⁷Li prefers the tetrahedral coordination in the melt over the octahedral coordination in tourmaline. At fluid saturation when melt and fluid separated, there appears to have been fractionation of the Li isotopes between them. Tourmaline in the pegmatitic zone is isotopically heavier (δ⁷Li = +13.4 to +22.9) than that in the pocket zone (δ⁷Li = +11.2 to +15.9). This suggests that ⁷Li was enriched in the melt and that the tetrahedral bonds of Li in the melt are stronger than the hydrated bonds of Li in the fluid. The δ⁷Li values in

tourmaline crystallized in the pocket are similar to those in the line rock tourmaline, which is consistent with the accumulation of the bulk of the initial Li that was in the original melt in the pocket fluid, as this would result in little change in the isotopic composition of the Li.

Introduction

The crystallization mechanisms of pegmatites is a highly debated topic (Jahns and Burnham, 1969; London, 1988; Morgan and London, 1999; Černý, 1991). Many hypotheses have been presented and include processes ranging from closed system fractional crystallization of hydrous melt (Jahns and Burnham, 1969) to rapid cooling completely to a glass with subsequent development of pegmatitic textures by zone refinement (Morgan and London, 1999). Černý (1991) described four plausible models for the development of pegmatites: 1) closed chamber crystallization, 2) open system deposition from flowing fluids, 3) recrystallization or metasomatism of finer-grained precursors, 4) metasomatic replacement by fluids generated in the pegmatite or introduced from an external source, or some combination of all of these. The prevalent view of the four presented by Černý (1991) is of crystallization of a volatile-rich, hydrous granitic melt under decreasing temperature in a relatively closed system with restricted exchange with the wall rock.

Jahns and Burnham (1969) presented a three-stage sequence of crystallization of a hydrous silicate melt in a closed system. The first stage involves crystallization of mostly anhydrous phases that can range in size from aplitic to pegmatitic. The second stage is the crystallization of a low viscosity-melt that coexists with exsolved aqueous fluid, leading to growth of very large crystals. The final stage is the crystallization of pocket minerals from a large vapor bubble in the absence of melt.

This study presents lithium concentrations and isotopic ratios in tourmaline from three pegmatitic dikes in San Diego County, California, that are used as indicators of

crystallization mechanisms of these pegmatites. Lithium is a trace-element in most granites, but is commonly extremely concentrated in many pegmatite dikes, which suggests that it plays an essential control in their petrogenesis. The extreme enrichments of Li in some pegmatites are evidenced by the occurrence of Li-rich minerals, such as elbaite tourmaline, spodumene, amblygonite-montebasite and lepidolite. Since Li can readily substitute into tourmaline, and tourmaline is a ubiquitous mineral in all portions of the pegmatite dikes, this study uses tourmaline as a proxy for lithium concentration in the dikes. Accordingly, tourmaline can be used as a recorder of a pegmatite's crystallization and the behavior of Li.

The idea of using tourmaline composition to trace crystallization processes is not unique to this study. Jolliff *et al.* (1986) used tourmaline compositions as a recorder of evolution of the large, zoned Bob Ingersol pegmatite in the Black Hills of South Dakota. They found a progressive decrease in Fe concentrations from the wall zone to the core of the pegmatite and a corresponding increase in Li, which they attributed to substitution of (Li + Al) for (Fe + Mg) in the structure of tourmaline with progressive crystallization. Jolliff *et al.* (1986) suggest that three crystallization processes leading to the formation of the Bob Ingersol pegmatite are distinguishable through compositional variation in the tourmaline. They are: 1) replacement of biotite during boron metasomatism in the country rocks leading to crystallization of a dravite-schorl tourmaline, 2) crystallization of an intermediate schorl tourmaline from a silicate melt in the wall zone, and 3) crystallization of elbaite in the core from a melt-aqueous fluid system.

The isotopic composition of the Li in the tourmaline can act as another indicator of crystallization processes. Lithium isotopes undergo extreme fractionation during

pegmatite crystallization and fluid exsolution due to the ~17% mass difference between the two isotopes ^6Li and ^7Li . Fractionation of Li is mostly controlled by the coordination of Li in minerals, fluids, and melts; the heavier isotope, ^7Li , prefers highly coordination states and stronger bonds, while ^6Li is fractionated into the weaker, lesser coordinated sites (Wunder *et al.*, 2007). For example, in the Tin Mountain pegmatite in the Black Hills, $\delta^7\text{Li}$ is higher in quartz than in plagioclase, muscovite, and spodumene, even though the concentration of lithium increases from plagioclase to muscovite to spodumene (Teng *et al.*, 2006). The isotopic composition of Li in individual minerals varies little, however, across the different pegmatite zones. The isotopic composition of fluid inclusions is also lighter than in quartz, and approximately the same as in muscovite and plagioclase. The elevated $\delta^7\text{Li}$ in quartz was attributed to ^7Li preferring the strong two- and four-fold sites in quartz over the weaker bonds in the other minerals and fluids. Teng *et al.* (2006) also suggested that minerals which crystallized in the presence of exsolved fluids, fluid-rich melts, or have re-equilibrated with late-stage fluids should be isotopically heavier than those that crystallized from a melt alone.

The goal of this study is to examine the relationship between Li concentration and isotope fractionation in tourmaline across pegmatite dikes in the San Diego pegmatite field in order to elucidate the interaction of minerals, melt, and fluid during crystallization.

Background Geology

The pegmatites of San Diego County, California, are located within the north-west trending, subduction-related Peninsular Ranges Batholith (PRB) that stretches from the San Jacinto Mountains into Baja California, Mexico. The PRB is bounded on the east by the San Andreas-Gulf of California Neogene transform-rift system and on the west by the Continental Borderlands (Wetmore *et al.*, 2003), and is the southernmost segment of North American Mesozoic Batholiths that stretch from Alaska to Baja California (Silver *et al.*, 1979) (Figure 1).

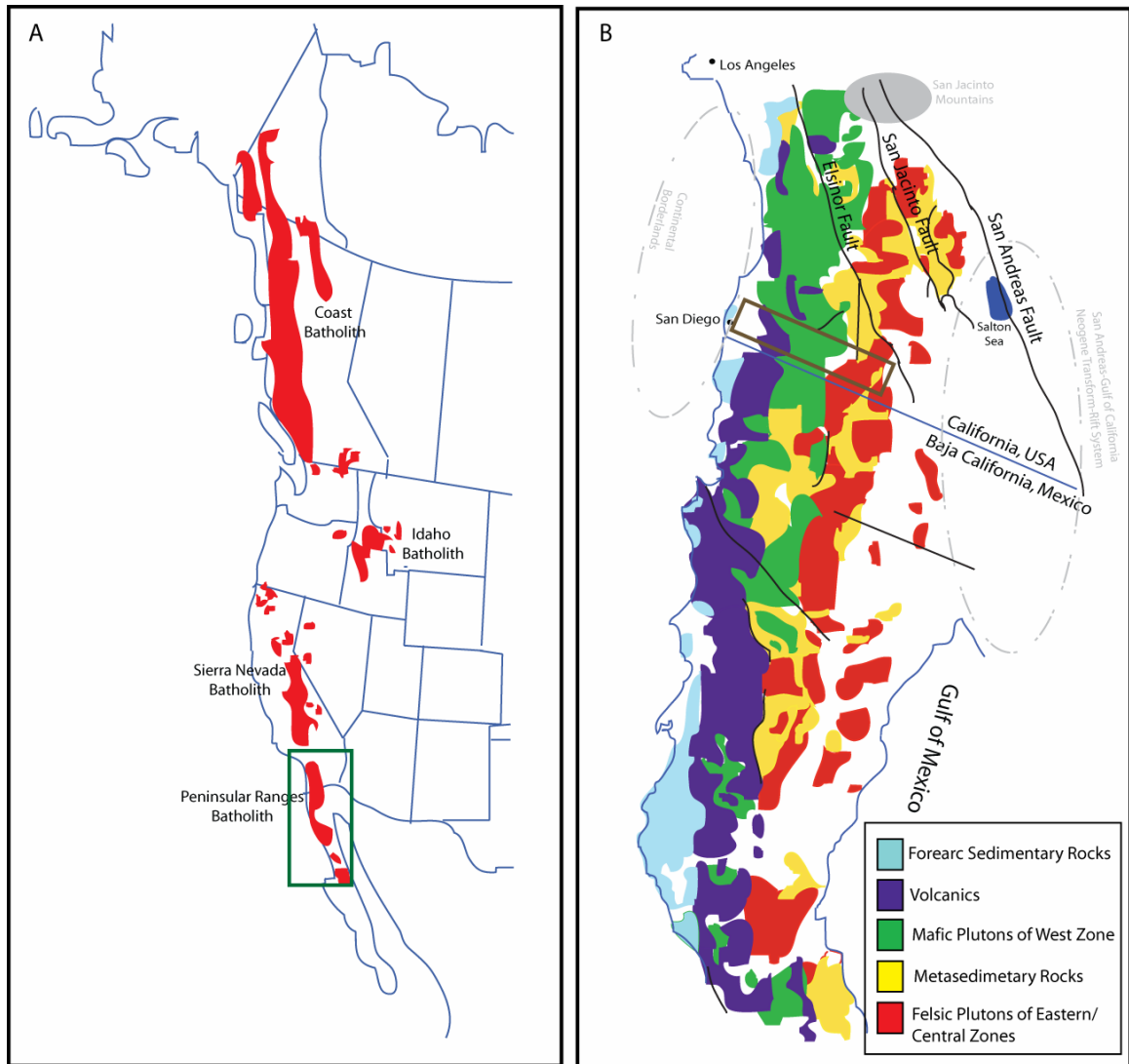


Figure 1: (A) North American Mesozoic Batholiths, figure B is highlighted in the box. (B) General geologic map of Peninsular Ranges Batholith, the study area in San Diego County, California, is highlighted in the box.

The PRB intrusive complex evolved as a continental margin migrating eastward across the pre-Triassic join between oceanic and continental lithospheres during subduction of the Farallon plate beneath the North American plate (Wetmore *et al.*, 2003). The batholith is divided into the western, eastern, and central zones based on

geochemistry, lithology, structure, and geophysics (Fisher, 2002; Clinkenbeard and Walawender, 1989, Silver *et al.*, 1979, Walawender, 1979, Gromet and Silver, 1979).

The western zone of the batholith is comprised of shallow I-type gabbros, quartz diorites, tonalites, granodiorites, and monzogranites ranging from 120 to 105 Ma intruded into late Jurassic to early Cretaceous basaltic to rhyolitic flows, volcanoclastic breccias, welded tuffs, and hypabyssal intrusions of the Santiago Peak Formation (Silver *et al.*, 1979, Walawender, 1979, Walawender *et al.*, 1990, Wetmore *et al.*, 2003). Post-tectonic pegmatites occur as late-stage dikes emplaced along cooling fractures in the gabbro and tonalite. Walawender *et al.* (1990) hypothesized that the western zone formed from subduction of partially altered oceanic crust, causing the release of volatiles that fluxed the overlying mantle wedge. This melting produced hydrous basaltic melts that rose to form gabbroic bodies in the oceanic lithosphere as well as the overlying sedimentary apron on the leading edge of the continent.

The more felsic eastern zone is dominated by large, concentrically zoned I- and S-type tonalites and monzogranites younger than 105 Ma intruded into greenschist to sillimanite-upper amphibolite facies metasedimentary rocks. In the study area, the plutons are intruded into the metasedimentary Julian Schist, metamorphosed Mesozoic sediments from a marginal basin that decrease in age (from late Precambrian to Cretaceous age) and metamorphic grade westward. (Clinkenbeard and Walawender, 1989, Walawender *et al.*, 1990, Wetmore *et al.*, 2003). The formation of the eastern zone plutons began ~105 Ma when magmatism in the western zone stopped due to a change in plate dynamics that caused shallower subduction. Walawender *et al.* (1990) suggest that the down-going slab was heated at a slower rate, and the volatiles released from the oceanic plate could no

longer escape into the water-saturated mantle wedge, so they caused partial melting of the down-going slab, as indicated by increased radiogenic Sr in the granites indicating an altered oceanic crustal source. The melts then rose and interacted with old continental crust and sedimentary rocks during emplacement.

The central zone is a belt of large, concentrically zoned granitic plutons with U-Pb emplacement ages between 90 Ma and 100 Ma (Symons *et al.*, 2003). Due to the similarity of the plutons in the central zone, they are commonly referred to as “La Posta-type plutons”, as the La Posta pluton is the largest pluton of this zone. La Posta-type plutons are defined as having concentric zoning with tonalitic margins and granodioritic/monzogranitic cores, gradational internal contacts, euhedral hornblende and biotite, large prismatic sphene, primary muscovite and biotite coexisting in the interior, megacrystic quartz and oikocrystic alkali feldspar also in the inner zones, and no foliation (Walawender *et al.*, 1990)

The La Posta pluton has a hornblende-biotite-sphene tonalite rim that grades to a muscovite-biotite granodiorite core. A layered border zone exists along contacts with older igneous rocks of the western zone and has alternating bands rich in hornblende, biotite, plagioclase and quartz (Walawender *et al.*, 1990). Potassium-argon cooling ages from hornblende and biotite decrease suddenly from ~100 Ma in the west to ~75 Ma in the east. These two zones are separated by a screen of the Julian Schist (Symons *et al.*, 2003, Walawender *et al.*, 1990).

San Diego pegmatite field

The San Diego pegmatite field consists of approximately 14 districts that define the suture between the two plutonic zones (Fisher, 2002) (Figure 2). The districts are defined by spatial relations, and the pegmatites show a surprisingly consistent structure from district to district. They are complex lithium-cesium-tantalum (LCT)-type granitic pegmatites, most of which are zoned with chemically, texturally, and mineralogically distinct hanging walls, footwalls, and pocket zones. From the hanging wall to the pocket zone, the grain size and the number of euhedral crystals increases. The hanging wall is typically characterized by an aplitic zone that coarsens to large euhedral K-feldspar crystals and then to graphic granite towards the central pocket zone (Jahns, 1979). The footwall is characterized by rhythmically layered aplite with oscillating changes in mineralogy from Mg-Fe-poor layers (quartz and albite) to Mg-Fe-rich layers (tourmaline or garnet), called “line rock”. Pocket zones, containing large euhedral, and sometimes gem and specimen quality crystals, are found in centers of the dikes.

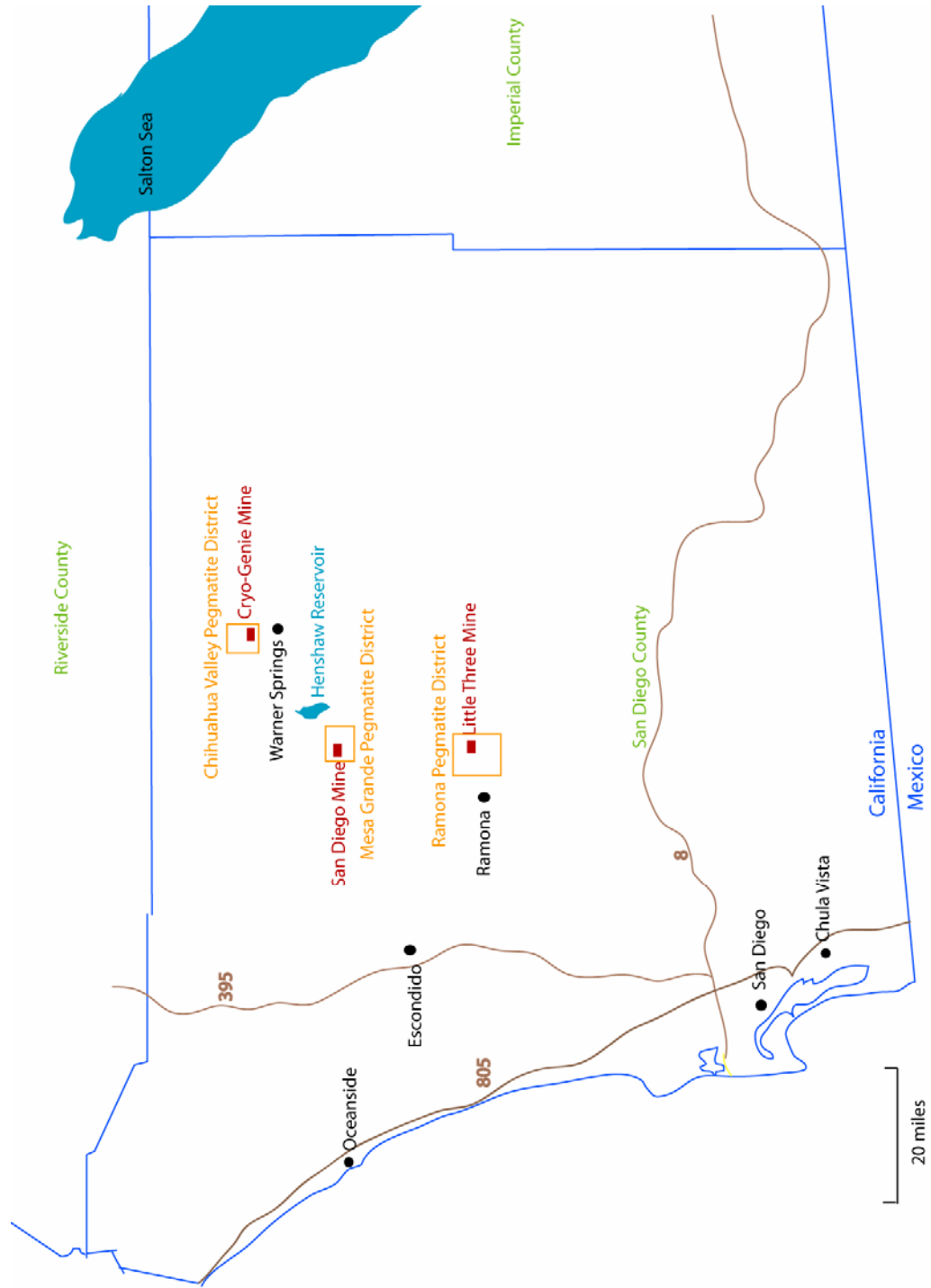


Figure 2: Map of San Diego County pegmatite districts.

Cryo-Genie

The Cryo-Genie mine is located just northwest of Warner Springs, CA, in the southern portion of the Chihuahua Valley pegmatite district. The pegmatite dike is intruded into sillimanite-grade metasedimentary rocks and the gneissic portion of the local La Posta-type biotite granite (Kampf *et al.*, 2003). The dike is possibly genetically related to younger two-mica granites that intrude the larger La Posta-type pluton. While no exact age has been measured for this dike, it is estimated to be 98-89 Ma based on field relations (Kampf *et al.*, 2003).

The dike strikes north-south, dips ~30° west, averages 2-4 m in thickness, and can be traced laterally for more than 200 meters (Kampf *et al.*, 2003). Ongoing mining operations have recovered large euhedral crystals of quartz, microcline, albite (var. clevelandite), elbaite, lepidolite, muscovite, and beryl. Gem and specimen quality elbaite and beryl (var. morganite) crystals have been recovered from the pockets. Samples for this study were collected along transects from the footwall to the hanging wall on the Green Ledge in the surface excavations and near the Payday Pocket in the underground workings.

Little Three

The Little Three mine is located in the Ramona Pegmatite district, in the central portion of San Diego County, just east of Ramona. The Little Three property contains five dikes: the Little Three main dike, the Hercules-Spessartine dike, the Spaulding dike, the Sinkankas dike, and the Hatfield Creek dike (Stern *et al.*, 1986). The dikes intrude into the Green Valley tonalite and gabbro, a member of the western zone of the PRB. The Little Three Mine is famous for its gem quality tourmaline and topaz, but each of the five

dikes is mineralogically distinct, especially in regard to pocket mineral assemblages (Stern *et al.*, 1986). The pockets of the Little Three dike consist of elbaite, muscovite or fluorine-rich lepidolite, quartz, microcline, albite, topaz, beryl, and hamgerite, the Hercules-Spessartine dike pockets contain muscovite, microcline, albite, spessartine, schorl, and quartz. The Spaulding dike pockets have produced orange garnet, smoky quartz, schorl, muscovite, biotite, albite, and K-feldspar; the Sinkankas dike pockets have produced hamberite; and the Hatfield Creek dike has yielded dark red-brown axinite (Stern *et al.*, 1986). Samples for this study were collected from the Little Three Main Dike as a nearly complete transect. Samples were also collected from a mineralized area of the Spalding dike.

Stern *et al.* (1986) described the mineralogical and geochemical evolution of the Little Three system as closed system crystallization in the presence of a hydrous silicate melt that evolved into a melt and coexisting aqueous fluid, and finally a supercritical fluid phase. Using experiments on a saturated halpogranite, Taylor *et al.* (1979) suggested that the Little Three dike was emplaced at temperatures ranging from ~700-730°C. Crystallization from a hydrous melt began with the aplitic footwall, through temperatures as low as 540°C. As crystallization progressed, the Na-rich albite crystallized from the residual melt while the exsolved fluid transferred K to the hanging wall. The subsequent nonequilibrium crystallization of the pegmatitic graphic granite zone occurred from a water-rich melt that was unsaturated to saturated with respect to water. Finally, the pocket zone crystallized from the exsolved aqueous vapor phase at temperatures 565-520°C or lower with the virtual absence of any melt.

San Diego Mine

The San Diego Mine is a member of the Mesa Grande pegmatite district centered on Gem Hill near Henshaw Reservoir (Fisher, 2002). The San Diego Mine exploits the Himalaya dike system: two N30W trending, 20-30°W dipping pegmatitic dikes hosted in the San Marcos Gabbro (Fisher *et al.*, 1999), medium to coarse-grained gabbro and norite (Jahns and Wright, 1951). The two dikes can be traced for 915 m along strike and are separated by 3 to 10 m north of the San Diego Mine, but converge on the mine property. The San Diego Mine is neighbored to the north by the Himalaya Mine (Webber *et al.*, 1999), a prolific producer of gem-quality colored tourmaline.

The two dikes formed during a single emplacement event at ~100 m.y. ago (Foord, 1976), as dated by fission track and K-Ar analyses. Well-crystallized specimens of perthitic microcline, albite (var. clevelandite), colorless and smokey quartz, tourmaline, beryl, lepidolite, stibiotantalite, hambergite, apatite, morganite, goshenite, and stilbite have been produced from this dike system (Fisher *et al.*, 1999). Samples were collected from an area where the two dikes converged in the underground workings of the San Diego Mine.

Methods

Bulk Li Concentrations

Tourmaline separates from three pegmatite localities in San Diego County, California, were ground in an automatic mortar and pestle until fine and homogeneous. 100 mg of each tourmaline was then fluxed with 400 mg of ground K_2CO_3 in an Al_2O_3 crucible at 500 °C in an oven. The temperature was slowly increased to 900°C and maintained there for 15 minutes, after which the furnace was turned off. The crucibles were cooled in the furnace overnight to negate cracking. The fluxed samples were washed into 15 ml centrifuge tubes using ~15 ml of 10% HNO_3 and centrifuged for 4 minutes. The liquid was decanted into Teflon beakers on a hot plate with an automatic stirrer. Another 15 ml of 10% HNO_3 was added to the remaining solid residue and the process was repeated. The remaining solid in the centrifuge tubes was finally dissolved in 3 ml of concentrated HNO_3 . This solution was added to the already dissolved fluxed tourmaline in the Teflon beakers and was stirred for at least 15 minutes on low heat. The samples were then brought up to 50 ml in a volumetric flask with 10% HNO_3 .

In several samples, a brown, amorphous precipitate formed after several days. After the liquid was decanted, the precipitate was dissolved in a combination of 1 ml of HF and 1 ml of HNO_3 in a small Teflon beaker with a screw top lid on a hot plate overnight. It was then brought up to 50 ml in a volumetric flask with distilled water. Analysis of the solutions revealed no Li.

Lithium and boron concentrations in the dissolved samples and precipitates were analyzed using the Perkin-Elmer Optima 3300 Inductively Coupled Plasma Optical

Emission Spectrometer (ICP-OES) at the University of Missouri-Columbia. Due to the high Li and B concentrations in tourmaline, synthetic standards were prepared to create the calibration curves for Li and B. Four solutions of K_2CO_3 were spiked with 0.05 ppm Li/5.00 ppm B, 0.10 ppm Li/10 ppm B, 1 ppm Li/15 ppm B, and 5 ppm Li/20 ppm B. Instrumental drift was accounted for by analyzing the prepared standards at regular intervals through the analysis and the solution of 1 ppm Li/ 15 ppm B was used as a check standard. Lithium and boron concentrations were obtained from the 610.362 nm and 249.772 nm emission lines, respectively.

Li isotope ratios

Analysis of Li isotopic ratios followed the procedures outlined in Teng *et al.* (2004) and Rudnick *et al.* (2004). The dissolved samples prepared for ICP-OES analysis were dried and prepared for determination of Li isotopic ratios at the Geochemistry Laboratory of the University of Maryland-College Park. Small portions of the dried samples were transferred to Savillex screw-top beakers and treated with a 3:1 HF-HNO₃ solution to remove silica. The samples were placed capped on a hot plate at ~90°C for one hour until all solids had dissolved; the resultant solutions were slightly cloudy due to the formation of fluorides. The samples were then uncapped and left on the hotplate to dry overnight. To redissolve the fluorides, the samples were treated with HNO₃, dried and retreated with HCl until the solutions were clear. The samples were dried once more to prepare for ion exchange chromatography.

Lithium separation was done using a three column technique based on that described by Moriguti and Nakamura (1998). Samples were dissolved with 2 ml of 4 M

HCl and centrifuged. The first of the three steps uses 12 ml polypropylene Bio-Rad columns filled with 1 ml of Bio-Rad AG 50Wx12 (200-400 mesh) resin; the resin was cleaned with 10 ml of 6 M HCl followed by 10 ml of milli-Q water. One milliliter of the sample was added to the first column, followed by 9 ml of 2.5 M HCl. Aftercut samples were collected using 2 ml of 2.5M HCl to determine if any Li was lost during separation. Each sample and its aftercut were dried overnight on the hotplate. The second separation uses the same columns and resin, but the dried samples were dissolved in 1.5 ml of 0.15 M HCl. This was added to columns that had been equilibrated with 1 ml of milli-Q water. The Li was collected using 30 ml of 0.15 M HCl and again placed on the hotplate to dry. The final Li separation was done using quartz-glass columns filled with 1 ml of the Bio-Rad resin that were equilibrated with 1 ml of milli-Q water. Since these columns were longer, a pressure head was applied using nitrogen gas. The samples were redissolved in 1 ml of 0.15 M HCl and added to the columns. The Li collection was done using 16.8 ml of 30% ethanol in 0.5 M HCl. The samples were placed on the hotplate to dry over night. Aftercuts were collected using 2 ml of the 30% ethanol in 0.5 M HCl mixture.

Before the analysis, the Na/Li ratios of the samples were evaluated semi-qualitatively. Any ratio larger than 5 causes interference in the Li isotope analyses, so samples with high Na/Li ratios need to be re-run through the third column. The purified Li solutions were diluted to ~100 ppb with 2% (v/v) HNO₃ and analyzed on a Nu Plasma Multicollector Inductively Couple Plasma Mass Spectrometer (MC-ICP-MS); ⁷Li and ⁶Li were measured simultaneously in separate Faraday cups (⁷Li in the high mass Faraday cup (H6) and ⁶Li in the low mass faraday cup (L5)). The samples were introduced to the Ar plasma using an ASX-100® Cetac Technologies auto-sampler then sent through an

Ardius® Cetac Technologies desolvating nebulizer fitted with a PFA spray chamber and Elemental Scientific micronebulizer. To ensure accuracy, each sample analysis was bracketed by measurement of the L-SVEC standard, each measurement of the $^7\text{Li}/^6\text{Li}$ of the L-SVEC had an average $2\sigma=0.003$. The $\delta^7\text{Li}$ of the samples were calculated relative to the average of the two bracketing L-SVEC runs. Two other Li-standards, IRMM-016 (Qi *et al.*, 1997) and the in-house standard UMD-1, were routinely analyzed during each analytical session. Two USGS rock standards, BHVO-1 (+4.2‰) and QLO-1 (+6.6‰), were analyzed for quality control purposes, both giving values in within the 2σ limit.

Results

The Li concentrations and isotopic compositions for tourmaline from dikes at the Cryo-Genie Mine, the Little Three Mine, and the San Diego Mine are presented in Table 1 and plotted in Figure 3.

Table 1: Lithium concentration and isotopic composition of tourmalines from Cryo-Genie mine (CG), Little Three mine (LT), and San Diego mine (SD), San Diego County, California.

Sample ID	Location	Li (ppm)	$\delta^7\text{Li}$
CG-1A	Pegmatitic Zone	53	+19.2
CG-1C	Pegmatitic Zone	174	
CG-1E	Pegmatitic Zone	138	
CG-1I BLACK	Pocket	273	+15.9
CG-1I GREEN	Pocket	5075	+14.7
CG-1N	Pocket	416	+11.2
CG-3E	Pocket	265	+16.1
CG-3I	Pocket	663	+11.2
CG-3K	Pocket	421	
CG-5B	Pegmatitic Zone	22	
CG-5D	Pegmatitic Zone	93	
LT-1G	Pegmatitic Zone	517	+13.4
LT-3F	Line Rock	56	+15.1
LT-3G	Line Rock	66	
LT-3I	Line Rock	70	+12.3
LT-4C	Pocket	268	+14.8
LT-5C	Pegmatitic Zone	452	+22.9
LT-5D	Pegmatitic Zone	113	+19.1
LT-5E	Pegmatitic Zone	135	+14.2
SD-4C	Pocket	954	+15.9
SD-2C GREEN	Pocket	1456	+13.7
SD-2C BLACK	Pocket	641	+15.9

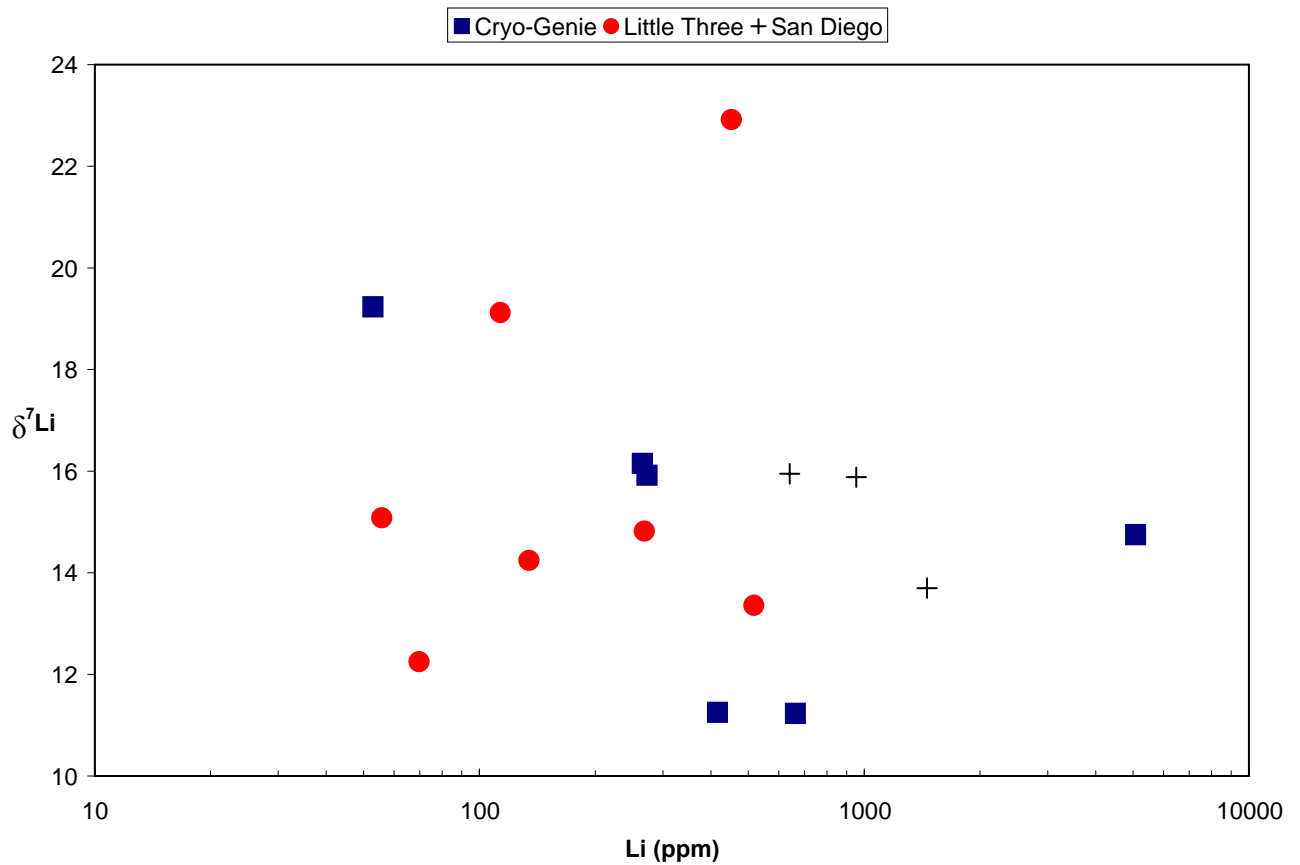


Figure 3: Plot of $\delta^7\text{Li}$ vs. ppm Li for all tourmaline samples. Data are from Table 1. Error bars are smaller than the symbol size.

There is a large range in Li concentration and isotopic ratios, but no systematic distinction in Li concentration or isotopic ratio between pegmatite districts, so it is best to examine the data in the context of individual dikes.

Cryo-Genie

A transect was collected across the Green Ledge dike from the hanging wall towards the pocket zone (Figure 4). This area was exposed by miners during surface mining by hand and using small explosives. Only the upper portion of the dike, from the

upper contact to the pocket, is exposed. The nearby “Green Ledge pocket” contained colored tourmaline and beryl (var. morganite).

Lithium concentrations in tourmaline range from 53 ppm to 5075 ppm, and increases from the wall rock contact towards the pocket zone. CG-1A is a sample of schorl taken from the hanging wall of the dike and has 53 ppm Li. CG-1C and CG-1E are larger euhedral schorl crystals collected from the pegmatitic layer below the graphic zone and have Li concentrations of 174 ppm and 138 ppm, respectively. Green and black tourmaline in the pocket commonly exhibit concentric zoning within individual crystals with black cores and green rims. Lithium concentration is correlated to tourmaline color, as shown by sample CG-1I. CG-1Iblack is the black core of a crystal that has 273 ppm Li, while the crystal’s green rim, CG-1Igreen, has 5075 ppm Li. Another black tourmaline collected from the pocket, CG-1N, has 416 ppm Li.

Lithium isotopic compositions also change between zones of the pegmatite and span the wide range from +11.2 to +19.2‰. Tourmaline CG-1A from the pegmatitic zone above the pocket is isotopically the heaviest with a $\delta^7\text{Li}$ of +19.2‰. Toward the dike’s center, $\delta^7\text{Li}$ decreases. The pocket minerals have the lightest Li with $\delta^7\text{Li}$ of +11.2, +14.7, and +15.9‰.

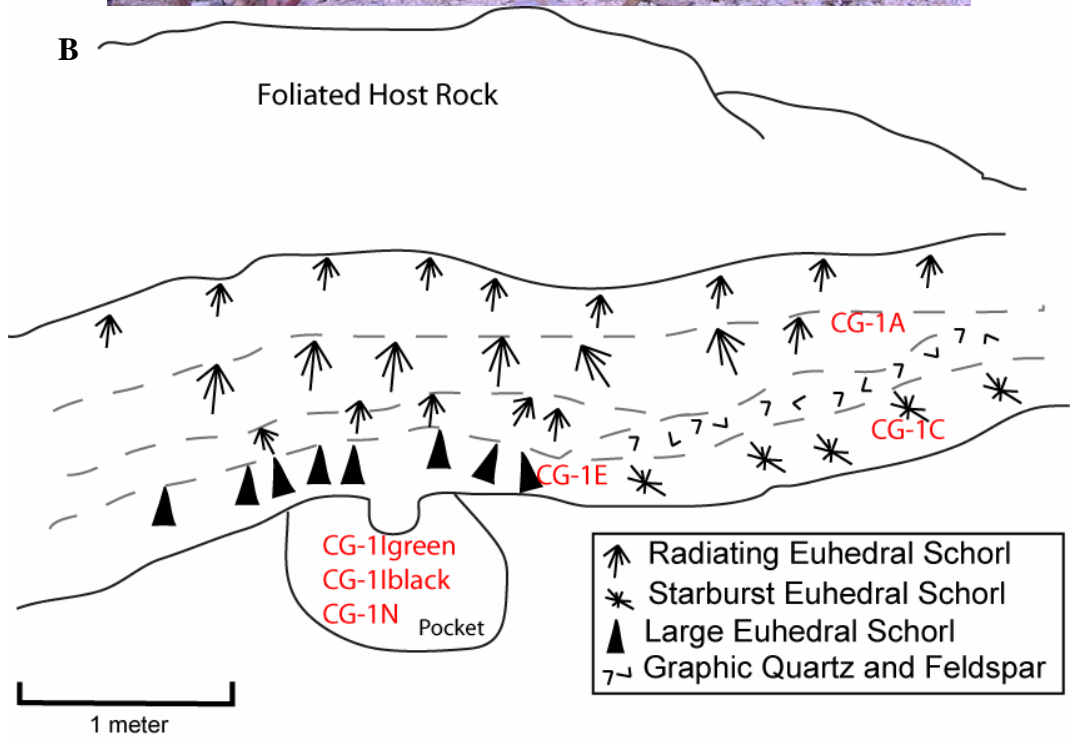


Figure 4: A: Picture of Jim Student, Peter Nabelek, and Mona Sirbescu in Green Ledge Pocket. B: Sketch of A, looking to the northeast

Samples CG-5B and CG-5D were also collected from the Green Ledge dike, but down dip from the above samples. A pocket in this area yielded only one large columbite crystal. The Li concentration in the tourmaline also increases from the wall rock contact towards the pocket, but there is a less dramatic jump at the aplite-pegmatite transition. CG-5B is a sample from the wall rock contact and has 22 ppm Li, whereas CG-5D, a tourmaline from the pegmatitic zone around the pocket has 93 ppm Li.

The Pay Day Pocket is located in the underground workings on the Cryo-Genie property (Figure 5). This pocket was opened in 2001 (Gochenour, 2003) and produced large green, pink, and black tourmalines. The dike is exposed from the aplite-host rock contact in the footwall to the pegmatitic zone above the pocket zone. All analyzed tourmalines from this location were from the pegmatite surrounding the pocket. The lithium concentrations of the tourmalines CG-3E, CG-3I, and CG-3K are 265 ppm, 663 ppm, and 421 ppm, respectively. They are within the range of those collected from the pegmatite pocket zone around the Green Ledge pocket.

The $\delta^7\text{Li}$ value for tourmaline CG-3K above the Pay Day pocket is +11.2‰, and is lighter than for tourmaline CG-3E in the bottom lining of the pocket, which is +16.1‰. Both of these values are lighter than the $\delta^7\text{Li}$ value of the wall zone tourmaline in the Green Ledge.

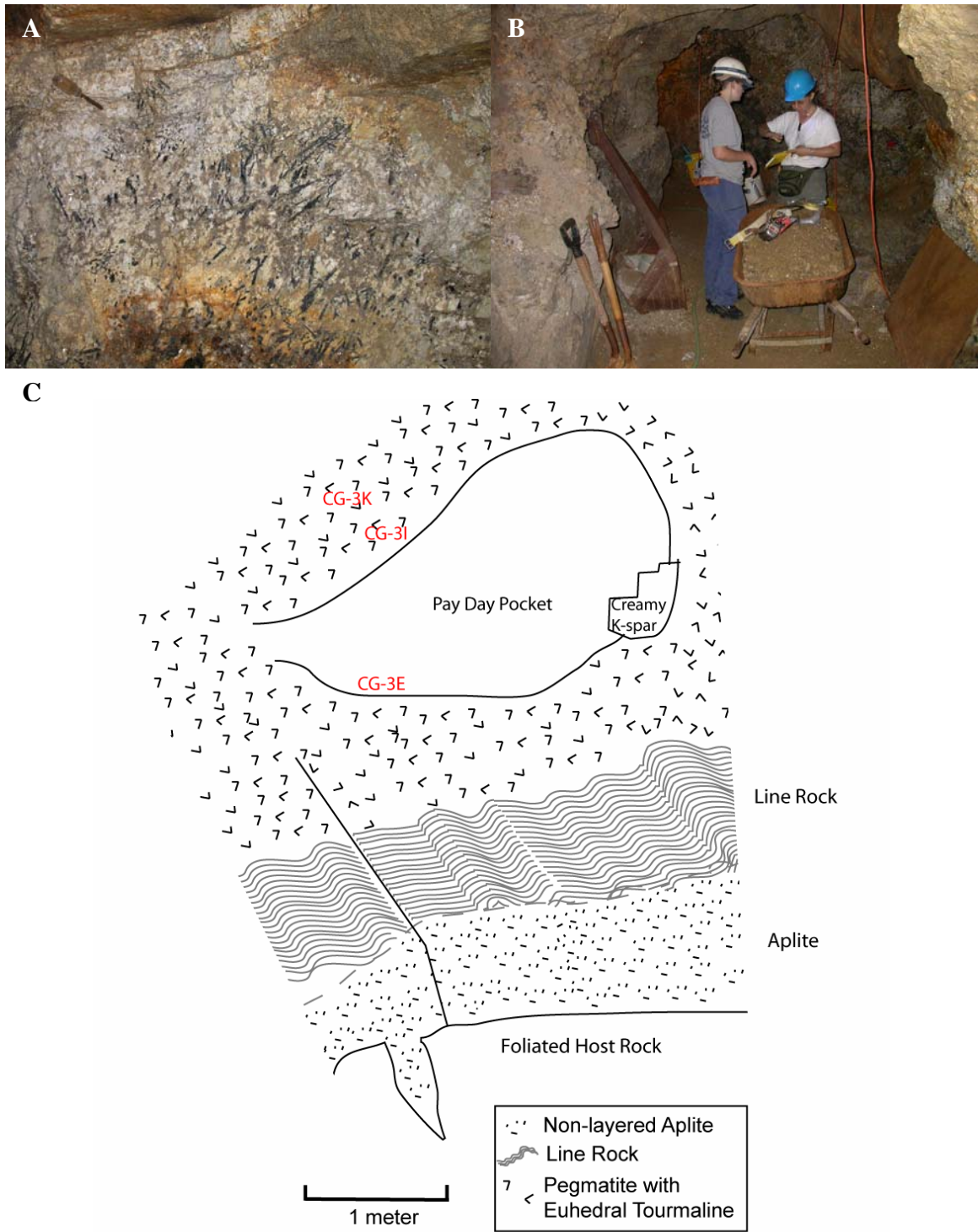


Figure 5: A: Photograph of pegmatite above Pay Day Pocket. B: Jennifer Maloney and Mona Sirbescu in underground workings of Cyro-Genie Mine. C: Sketch of the Pay Day pocket in the underground workings of the Cryo-Genie mine, looking north.

Little Three

The Little Three main dike has been the largest producer of gem quality tourmaline on the Little Three property. Samples were collected just outside the mine entrance on the Topaz Ledge. This dike consists of two zoned pulses separated by a thin chilled margin (Figure 6). The bottom pulse has a wavy aplitic contact with the host tonalite that coarsens upward to a pegmatitic zone. Above the pegmatitic zone is distinct line rock below a chilled margin. The line rock oscillates between tourmaline rich layers and quartz and feldspar rich layers. The larger upper pulse sits on top of the first and has line rock with the same mineralogy of the lower pulse in its bottom portion. The line rock terminates sharply at the pegmatitic zone which consists of large euhedral tourmaline and graphic quartz and feldspar intergrowths. The pocket zone sits in the middle of the pegmatitic zone. The hanging wall has biotite books growing down from the upper contact.

Tourmalines LT-3F and LT-3G were separated from the line rock of the upper pulse. LT-3F is at the very bottom of this line rock zone, in contact with the chilled margin, and has 56 ppm Li. LT-3G is from the middle of the line rock zone and has 65 ppm Li. Tourmaline LT-3I is from the top of line rock of the lower pulse. Its Li concentration is 70 ppm.

Lithium isotopic composition of tourmaline in the line rock is consistent relative to tourmaline in the wall rock contact of the Cryo-Genie mine. LT-3F from the bottom of the upper pulse has a $\delta^7\text{Li}$ of +15.1‰ while LT-3I from the top of the line rock in the lower first has a $\delta^7\text{Li}$ of +12.3‰.

Directly above the Topaz Ledge mine entrance is the Dave London 1991 pocket. One large tourmaline that grew down from the roof of this pocket, LT-4C, was analyzed. The Li concentration is consistent with other black pocket tourmalines, 268 ppm. The $\delta^7\text{Li}$ of this tourmaline is +14.8‰.

Samples were also collected from the southern end of the mineralized section of the Topaz Ledge. This is a large area of pegmatite with smaller blocks of line rock that sit above an exposed pocket floor. It is possible that these blocks of line rock were rafted into the pegmatitic portion of this dike. LT-5C, LT-5D, and LT-5E were collected from the pegmatitic portion in contact with one of the line rock blocks. The tourmalines have concentrations of 452 ppm, 113 ppm, and 135 ppm Li, respectively. The concentrations of LT-5D and LT-5E are consistent with those of euhedral tourmaline from the pegmatitic portion of the dike at the Cryo-Genie mine (53 to 174 ppm), but LT-5C has significantly more Li.

The $\delta^7\text{Li}$ values are +22.9‰ for LT-5C, +19.1‰ for LT-5D, and +14.2‰ for LT-5E. This Li is heavy compared to Li in similar tourmalines from other dikes and are more comparable to tourmalines from wall rock-aplite contacts than those in pegmatitic portions.

One sample was collected from the Spalding Dike, along the Garnet Ledge. This was a trench in surface workings that yielded large orange garnet crystals. A tourmaline from this location, LT-1G, had 517 ppm Li and a $\delta^7\text{Li}$ of +13.4‰.

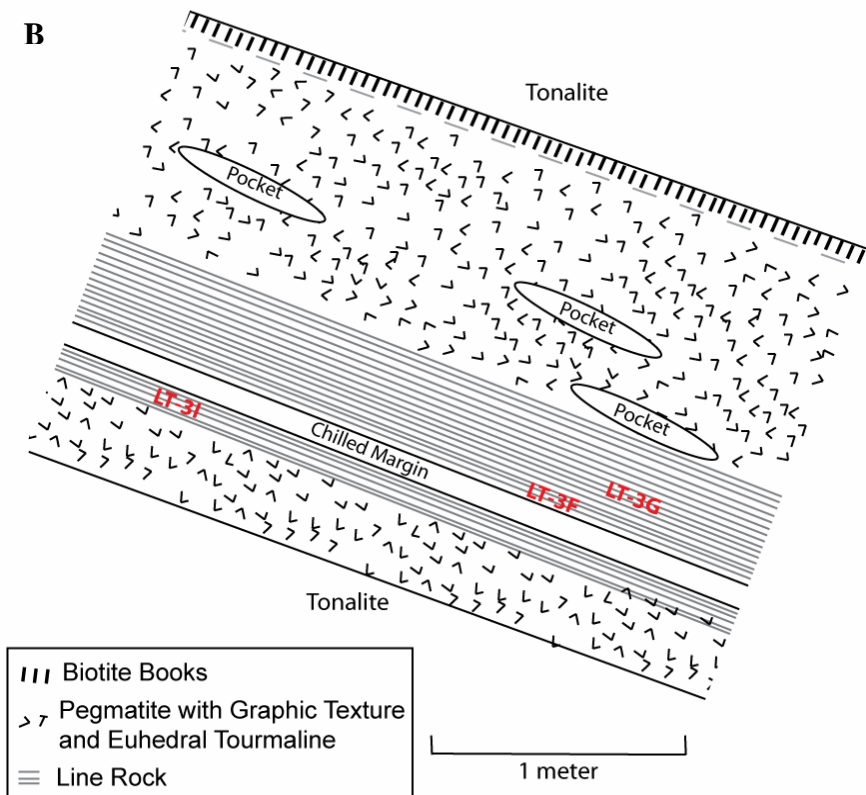


Figure 6: A; Photo of the upper pulse of the Little Three Main Dike at the Topaz Ledge B. Sketch of Topaz Ledge e outside the entrance to the mine of the Little Three main dike, looking north.

San Diego

A euhedral, concentrically zoned tourmaline with a black core, SD-2Cblack, and a green rim, SD-2Cgreen, from a probable pocket in the San Diego mine was analyzed. The black core has 641 ppm Li with $\delta^7\text{Li}$ of +15.9‰. The green rim of the crystal has 1456 ppm Li with $\delta^7\text{Li}$ of +13.7‰. SD-4C, a black tourmaline crystal, was collected from a small productive pocket of the mine. This sample has 954 ppm Li with $\delta^7\text{Li}$ of +15.9‰.

Summary

Since Li is a characteristic element in the San Diego LCT-type pegmatite dikes, Li concentrations and isotopic ratios in tourmaline have the potential to serve as indicators of pegmatite crystallization and the conditions under which different zones crystallize. Tourmaline in aplitic zones and line rock in contact with host rocks has the lowest concentration of lithium, on the order of tens of ppm (Figure 7). There is a significant jump in Li concentration between tourmaline in line rock or aplite and euhedral tourmaline in the pegmatitic zones of the dikes, which typically have Li concentrations in excess of 100 ppm. Black schorl tourmalines in pockets have similar concentrations while green rims have concentrations ranging to thousands of ppm.

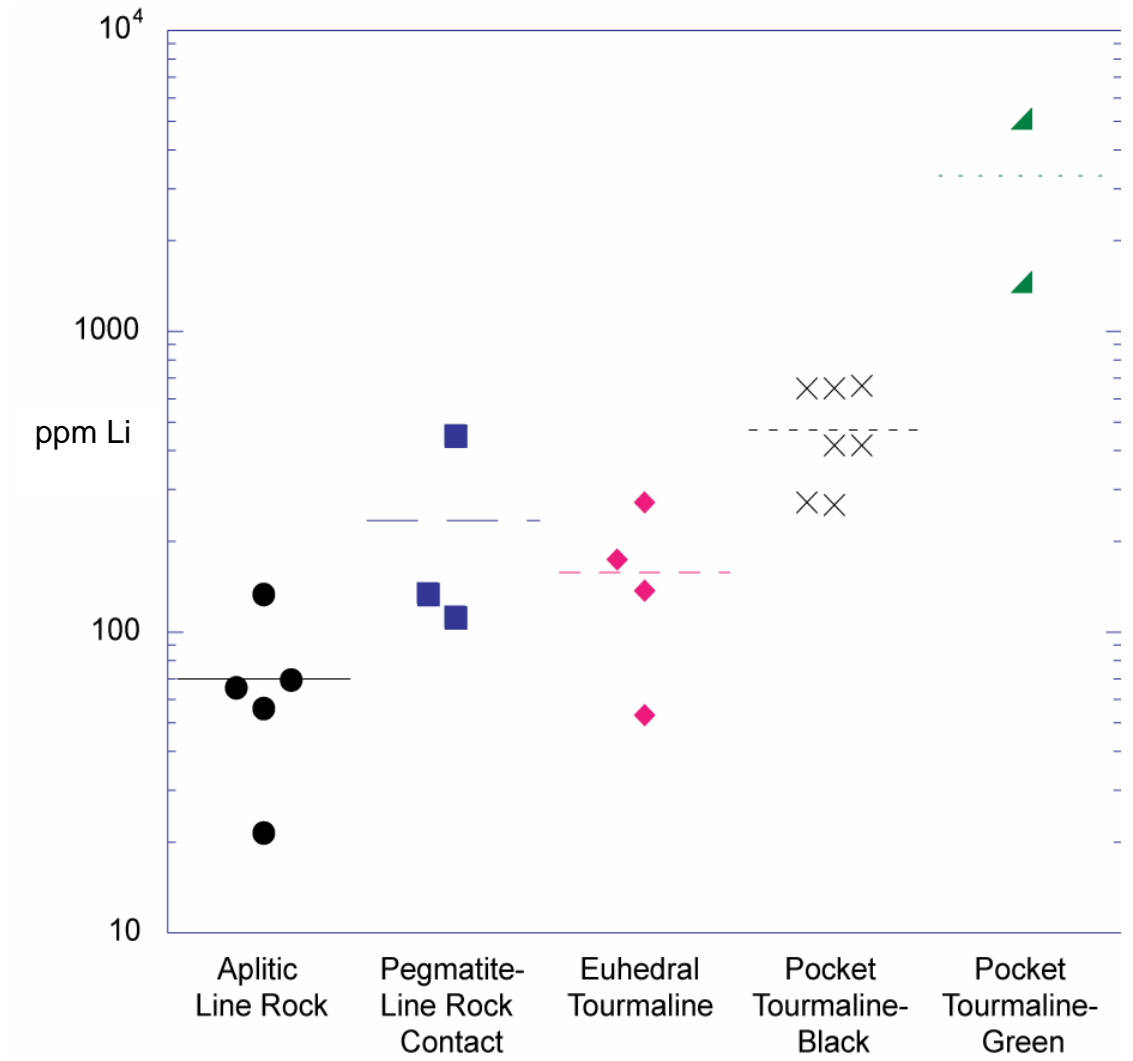


Figure 7: Li concentration in tourmaline found in different zones of the San Diego County Pegmatites. Horizontal lines represent average concentrations for each zone. Error bars are smaller than the symbol size.

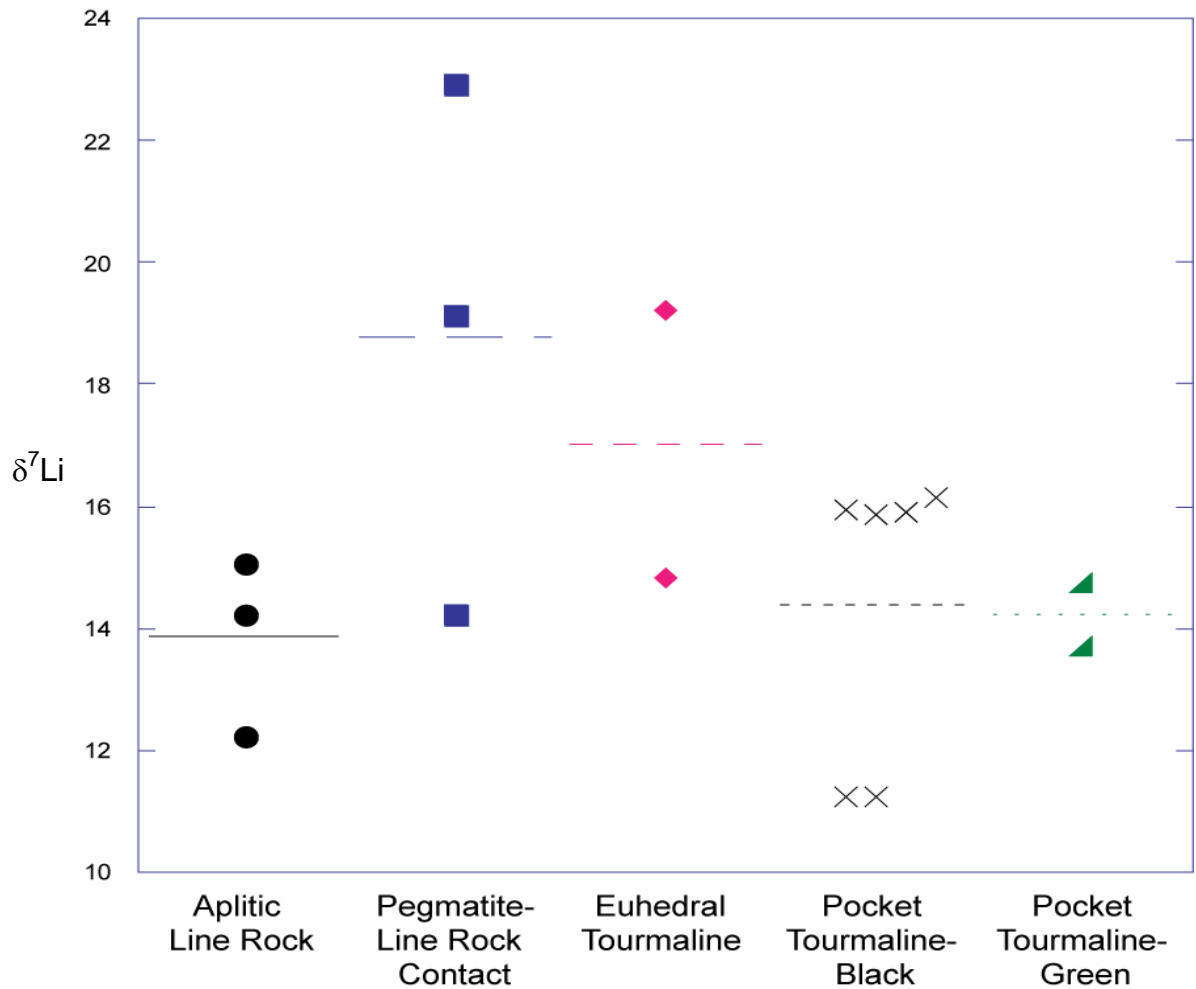


Figure 8: $\delta^7\text{Li}$ for tourmalines found in different zones of the San Diego County Pegmatites. Horizontal lines represent average $\delta^7\text{Li}$ values for each zone. Error bars are smaller than the symbol size.

Lithium isotope ratio changes correlate with jumps in Li concentration across zones, but the relationship is not simple (Figures 7 and 8). The lowest $\delta^7\text{Li}$ is in aplite and line rock tourmaline that has the lowest Li concentrations. The jump in Li concentration at the line rock- pegmatite border is accompanied by a sharp increase in the average $\delta^7\text{Li}$. The pocket tourmaline has on average about the same Li isotope composition as in the aplitic zone, but has the highest Li concentration. It is notable that the green rims of pocket tourmalines are isotopically lighter than the corresponding cores.

Discussion

Lithium is enriched in L-C-T pegmatites, and in the San Diego County pegmatites Li is stored in almost exclusively in tourmaline and in the pockets also in lepidolite. The absolute Li concentration varies between zones of the dikes showing progressive enrichment from the line rock border zones to the pockets. Due to high Li concentrations in the dikes and the ability of tourmaline to incorporate extreme amounts of Li into its structure, Li concentration in tourmaline can serve as a mirror on the pegmatite crystallization process.

Lithium Concentration and the Crystallization Process

Tourmaline in the line rock has the lowest concentration of Li compared to tourmaline in other zones. This suggests that during line rock crystallization, Li was incompatible with respect to minerals in the line rock, including tourmaline. Euhedral tourmaline in the pegmatitic zones contains more Li than tourmaline in the line rock, but much less Li than tourmaline in the pockets. The high concentration of Li in the pocket resulted in the crystallization of elbaite (Li-rich tourmaline end-member), and is supported by the high concentration of Li in fluid inclusions (~9100 ppm; Sirbescu, pers. comm.) in quartz that formed on the pocket floor.

The difference in Li concentration between tourmaline in the pegmatitic zones and in the pockets suggests that Li was partitioned between pegmatite and fluid at the point of fluid saturation in the melt (Figure 10). Fluid saturation of the melt is marked by the change in texture from the aplitic line rock to the very coarse grained pegmatite. It is suggested that the large crystals in the pegmatite formed as the result of H₂O acting as a

network-modifier in the melt, which results in lowering of melt viscosity and in increasing the diffusion rate of chemical components, which allow faster crystal growth, even at low temperatures of undercooling. Two-feldspar thermometry records crystallization temperatures of the melt as low as 240°C in the Little Three dike, which probably cooled to below its solidus in 33-84 days (Morgan and London, 1999). The possibility of very low crystallization temperatures of pegmatite dikes to <350° C is supported by microthermometry of primary fluid inclusions in the Tin Mountain pegmatite in the Black Hills, oxygen isotope ratios in coexisting quartz and K-feldspar and lack of tartan twinning in K-feldspar, which indicate its subsolvus crystallization (Sirbescu and Nabelek, 2003).

The extremely high Li concentrations in the pockets suggest that most of the Li partitioned into the fluid. In a hydrous, peraluminous composition, Li is an incompatible element with a $D^{fluid/melt} \sim 0.4$ at temperatures ranging from 650 to 775°C (London *et al.*, 1988). Webster *et al.* (1989) suggested that $D^{fluid/melt}$ increases with temperature, mole fraction of water, and Cl content in the vapor.

The enrichment in incompatible Li from the wall zones towards the pocket indicates that the dikes crystallized inward from the wall rock contact. It is suggested that line rock crystallized until the melt reached fluid saturation, at which point fluid and the melt separated to form the pegmatitic zones and the pockets, respectively. These trends support the Jahns and Burhnam (1969) hypothesis of pegmatite formation through fractional crystallization and vapor separation in a hydrous melt. The Li enrichment observed in the San Diego County pegmatites is inconsistent with pegmatite development

by open system deposition from flowing fluids, metasomatism of finer-grained precursors, or zone-refining of a rapidly quenched melt.

Initial Lithium Concentration of the Melt

In order to determine the amount of enrichment of potential fluxing components that occurs during pegmatite crystallization, the initial concentration (C_0) of Li in the melt was estimated from concentrations found in tourmaline and fluid inclusions. The initial Li concentration can be accounted for by the mass proportion of line rock, pegmatitic zone, and fluid bubble (now represented by the pocket). As tourmaline is the largest reservoir for Li in the dike, the concentration of Li in line rock and pegmatite can be estimated by the proportion of tourmaline in each zone and the amount of Li in the tourmaline (Table 2). The Li concentration in the fluid bubble was determined by analysis of primary fluid inclusions in quartz that occurs in or near the pockets. These inclusions have on average ~9100 ppm Li.

Using the mass balance equation:

$$C_0 = X_{LR}C_{LR} + X_{PEG}C_{PEG} + X_{POCK}C_{POCK},$$

where X is the mass proportion of each zone and C is the concentration of Li in each zone (Table 2), the initial concentration of Li in the melt was calculated as ~1120 ppm. Most of this Li is in fact accounted for by Li in the pocket fluid. Given a leucogranite composition of the melt with 5 wt% H_2O , as estimated to be water-saturation at 2 kbar emplacement, the pegmatitic melt is estimated to have initially contained ~0.5 mol % Li_2O (Table 3).

The concentration of Li in these pegmatites is significantly higher than that in granites. The Harney Peak Granite in the Black Hills of South Dakota contains 10's of ppm Li in areas of the pluton devoid of pegmatites and 100's of ppm in pegmatitic portions (Nabelek, unpublished data). In contrast, the Tin Mountain pegmatite, contains up to 1.7 wt % Li₂O (Walker *et al.*, 1986). This elevated Li content is manifested in the pegmatite by the presence of extremely Li-rich mineral phases, such as spodumene and amblygonite.

Many crystallization processes for Li-rich pegmatites have been proposed and differ significantly (Walker *et al.*, 1986; Morgan and London, 1999), but all hypotheses suggest that Li has a large influence on the behavior of the melt. Walker *et al.* (1986) hypothesized that crystallization of the Tin Mountain pegmatite commenced in the wall zone, based on the low Li concentrations in the wall zone. The first intermediate zone crystallized next, marked by the high Sr concentration and positive Eu anomaly in the feldspar. The structure of the melt then changed when it became more fluid rich and the core, 2nd, and 3rd intermediate zones crystallized simultaneously inward.

Morgan and London (1999) propose a vastly different crystallization process for the Little Three Pegmatite. Morgan and London (1999) hypothesized that the low temperature and the fast cooling rate that must have occurred during solidification of the pegmatite did not allow for crystal nucleation until the melt has reached a state of very large undercooling (~250°C below the equilibrium liquidus). They proposed that the dike quenched to a glass and that crystals formed through constitutional zone refinement – a F and Li-rich boundary layer that formed due to the large initial undercooling, rapid growth rate, and low temperature impeded diffusion of incompatible elements into the melt,

which migrated through the glass. The increase of Li in the pocket zone of the Little Three was therefore suggested to be due to an increase in incompatible Li in the boundary layer as it moved through the dike and culminated near the pockets.

It is proposed here that the crystallization of the San Diego County pegmatites does not occur by constitutional zone refinement, but by crystallization from a highly fluxed melt, similar to the process suggested by Walker *et al.* (1986). The presence of fluxing components in high concentrations in pegmatitic melts, such as Li and H₂O, alter the rheology of a silicate melt by depolymerizing the silicate network (Mysen and Richet, 2005). In natural melts, oxygen in the SiO₄ tetrahedra can bond with the cation or water molecule, depolymerizing the melt.

The effect on melt polymerization, and therefore properties directly dependent on polymerization such as viscosity and diffusivity, increases with concentration of fluxing components. The presence of Li alone in the melt lowers the viscosity of the melt, but it is doubtful that 0.5 mole % of Li₂O alone would have had a drastic effect on the properties of the pegmatitic melts. Pegmatitic melts are also hydrous, and the presence of water in the melt has an even greater effect on the structure of melt than Li. Water depolymerizes the melt by dissolving as molecular H₂O and OH⁻ groups. The OH⁻ groups can form alkali-OH, Al-OH, and Si-OH complexes which break up the tetrahedral network. For example, in alkali-bearing melts, viscosity drops dramatically with in the first 1 wt% water (Romano *et al.*, 2001). This drop in viscosity promotes a faster diffusion rate and faster crystal growth. Water also depresses the solidus and glass transition of the melt to allow for crystallization of a strongly undercooled melt, negating the necessity of a dike solidifying to glass at temperatures <400°C (Morgan and London,

1999). In a haplogranite, the glass transition temperature (T_g) is depressed $>350^\circ\text{C}$ with the addition of 5 wt.% H_2O (Dingwell *et al.*, 1996), and for a peraluminous leucogranite, Whittington *et al.* (2004) showed that T_g was reduced from 766°C to 414°C with the addition of 3.4 wt.% H_2O . This depression of T_g allows for the crystallization of fluxed undercooled liquids before viscosity increases and crystal growth becomes hindered as the melt approaches the glass transition.

Pegmatitic melts are also enriched in F, as evidenced by the crystallization of tourmaline, topaz, and minor fluoroapatite. The presence of F in the melt reduces viscosity, and has an increased effect with increasing SiO_2 content of the melt. F substitutes for a bridging oxygen forming Si-F bonds, and also forms complexes with Al in a non-network position, liberating equivalent alkalis, such as Li, from charge balancing roles, depolymerizing the melt (Mysen and Richet, 2005).

Table 2: Mass balance data for C_o(Li) of pegmatitic melt.

Line Rock	ppm Li	% Tour	C _{LR}	Euhedral Tour	ppm Li	% Tour	C _{PEG}
LT-3I	70.0		5	CG-1A	52.9		5
LT-3F	55.8		5	CG-1C	173.9		5
LT-3G	65.6		5	CG-1E	137.8		5
Average			3.2	LT-4C	268.3		5
				Average			7.9

Inclusion Chem	Li/Cl Wt.	C _{POCK}	Average Salinity
05CG-1L	0.362	7078.614	19546 ppm Cl
05CG-1M	0.439	8574.499	ρ _(H₂O) 2Kbar
05-CG-1N	0.607	11868.297	2wt% Cl
Average		9173.8	300 kg/m ³
			2700 kg/m ³

(M.-L. Sirbescu, pers.comm)

V Line Rock	
V Pegmatite	0.34
V Pocket	0.57
	0.09

(Jahns and Burnham, 1969; estimated from field observations and image analysis)

$$C_o = X_{LR}C_{LR} + X_{PEG}C_{PEG} + X_{POCK}C_{POCK}$$

$$X_{LR} = \frac{\rho_{granite}}{(V_{LR} \times \rho_{granite}) + (V_{PEG} \times \rho_{granite}) + (V_{POCK} \times \rho_{fluid})}$$

$$X_{PEG} = \frac{\rho_{granite}}{(V_{LR} \times \rho_{granite}) + (V_{PEG} \times \rho_{granite}) + (V_{POCK} \times \rho_{fluid})}$$

$$X_{POCK} = \frac{\rho_{fluid}}{(V_{LR} \times \rho_{granite}) + (V_{PEG} \times \rho_{granite}) + (V_{POCK} \times \rho_{fluid})}$$

Table 3: Tourmaline granite composition from Black Hills, South Dakota normalized to 5% H₂O with calculated wt% Li₂O.

	Wt% Oxide	Mol % Oxide
SiO ₂	73.6	67.71
TiO ₂	0.2	0.14
Al ₂ O ₃	15.2	8.24
FeO	0.8	0.62
MnO	0.07	0.05
MgO	0.1	0.14
CaO	0.6	0.59
Na ₂ O	4.7	4.19
K ₂ O	3.1	1.82
P ₂ O ₅	0.2	0.08
H ₂ O		15.96
Li ₂ O	0.241	0.46
Total	98.57	100.00

Lithium Isotopic Fractionation

A potentially large fractionation of Li-isotopes in any multiphase system is owed to the 17% mass difference between ⁷Li and ⁶Li. Fractionation of Li isotopes in igneous systems can occur during partial melting, fractional crystallization and fluid exsolution (Teng *et al.*, 2006). Because fractionation of isotopes of light elements among phases is usually temperature-dependent, fractionation also may be enhanced by cooling. In crystallizing magmatic systems in the presence of aqueous fluids, e.g. pegmatitic dikes, the main control on Li isotope fractionation is the coordination state of Li, however. The lighter isotope (⁶Li) preferentially occupies sites with higher coordination numbers, and

therefore, weaker bonds, while the heavier isotope (^7Li) prefers phases with smaller coordination numbers and stronger bonds (Wunder *et al.*, 2007).

Fractionation of Li between minerals and fluids has been experimentally determined only for a very limited set of minerals (Wunder *et al.*, 2007; Lynton *et al.*, 2005). Wunder *et al.* (2007) experimentally determined the fraction of lithium between staurolite and fluid and mica and fluid through a range of P and T conditions, and obtained an average $\delta^7\text{Li}_{\text{staurolite-fluid}} = +1.3\text{‰}$. This value is not significantly temperature-dependent but it indicates that ^7Li has a slight preference for staurolite over the fluid. For Li-bearing muscovite, the fractionation of Li isotopes is temperature-dependent and decreases with increasing temperature. At temperatures of 350, 375, and 400 $^\circ\text{C}$, the mean values of $\Delta^7\text{Li}_{\text{mica-fluid}}$ are -2.55‰ , -2.15‰ , and -2.00‰ , respectively.

For both minerals, Wunder *et al.* (2007) conducted experiments in the presence of LiCl and LiOH-bearing fluid. At any given temperature, fractionation was insensitive to fluid composition, which implies that Li-complexation in the two fluids was not different. In aqueous solutions, Li appears to form a tetrahedrally coordinated hydrated ion, $[\text{Li}(\text{H}_2\text{O})_4]^+$, not LiCl or LiOH complexes as assumed in previous studies (Lynton, 2005) or suggested by Webster *et al.*'s (1989) experiments. Isotopic fractionation is then controlled by Li-coordination with ^7Li preferentially incorporated into the phase which allows for a smaller coordination number. In staurolite, Li substitutes for the divalent cations Fe^{2+} , Mg, and Zn in the tetrahedral site of the structure. In muscovite, however, Li exists as an octahedrally coordinated cation between the silicate layers, thus the larger preference of $\delta^7\text{Li}$ for staurolite over muscovite.

Tourmaline, $XY_3Z_6Si_6O_{18}(BO_3)_3(OH,O)_3(OH,F,O)$, (Figure 9) occurs in granitic rocks with compositions ranging from the Fe-bearing schorl, $(NaFe_3Al_6Si_6O_{18}(BO_3)_3(OH)_3(OH))$ end member, to the Li-bearing elbaite, $(NaLi_{1.5}Al_{1.5}Al_6Si_6O_{18}(BO_3)_3(OH)_3(OH))$ end member (Deer *et al.*, 1992, Hawthorne and Henry, 1999). The approximately linear variation between schorl and elbaite can be described by the coupled substitution $2^YFe^{2+} \rightarrow ^YAl^{3+} + ^YLi^+$ (Bosi *et al.*, 2005; Hawthorne and Henry, 1999). Schorl is the major composition throughout the pegmatite while elbaite is found almost exclusively in the pocket.

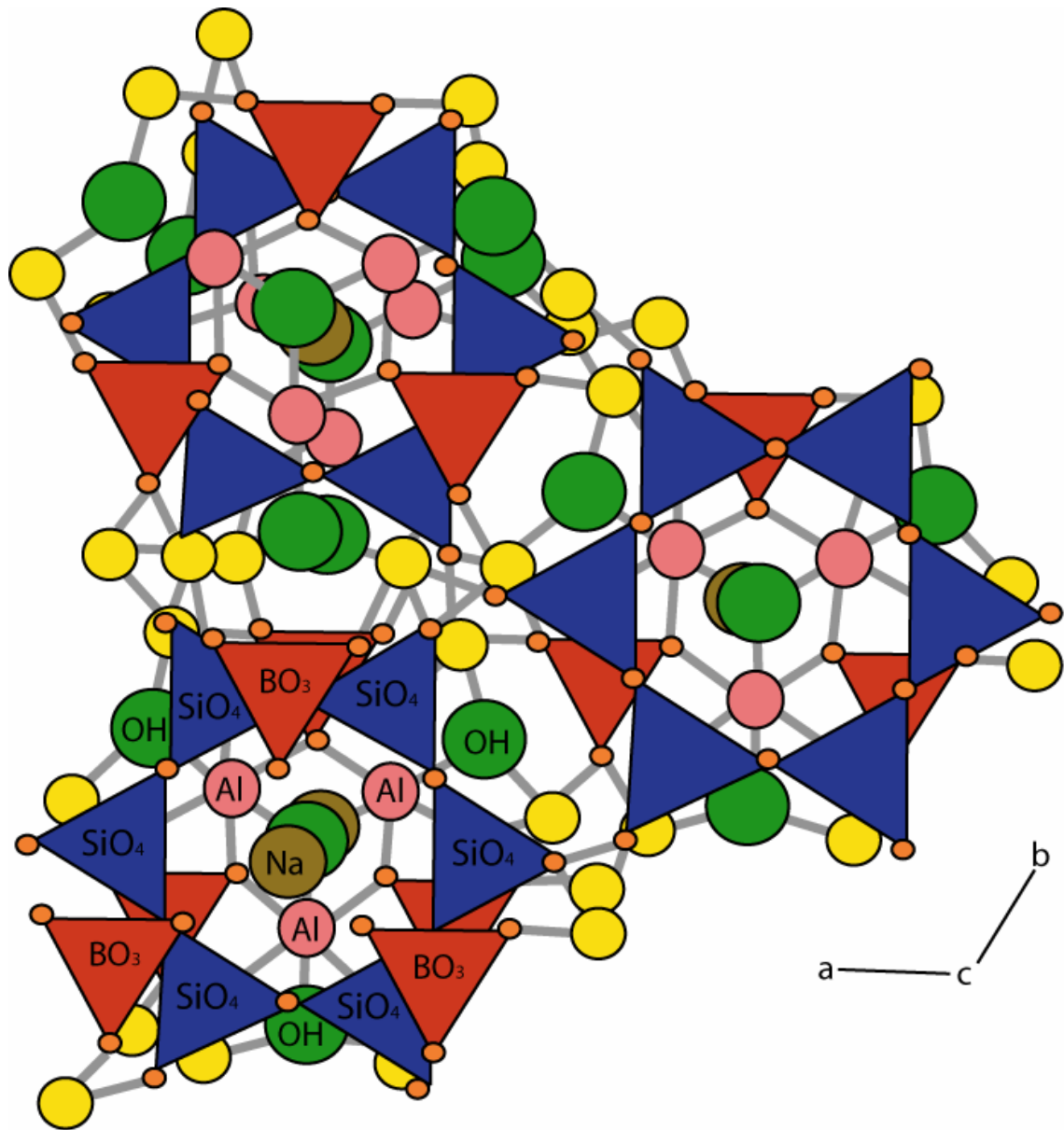


Figure 9: Tourmaline crystal structure. Small orange circles represent O^{2-} , and yellow circles represent cations in the Y-site: Li^+ , Fe^{2+} , Fe^{3+} , Mg^{2+} , or Al^{3+} . In schorl, the Y-sites are filled with Fe^{2+} and Fe^{3+} . In elbaite, the Y-sites are filled with Li^+ and Al^{3+} . The brown circles represent the X-site filled with Ca^{2+} , Na^+ , K^+ , or a vacancy. The pink circles represent the Z site filled with Mg^{2+} , Al^{3+} , Fe^{2+} , Fe^{3+} , Cr^{3+} , or V^{3+} . (Hawthorne and Henry, 1999, Perkins, 2002)

The pegmatitic dikes of San Diego County, California, were a system of coexisting minerals, melt, and fluid, in each of which Li was in a different coordination state. In tourmaline, Li occupies the octahedrally coordinated Y-site. In the melt,

however, Li is in a charge balancing role, balancing Al^{3+} , in a peraluminous melt as $\text{LiAlSi}_3\text{O}_8$ (Mysen and Richet, 2005). Li is probably very strongly bonded in the charge balancing site in the alumino-silicate melt.

The isotopic composition of Li in tourmaline in the San Diego pegmatite dikes is reflective of the medium from which the tourmaline crystallized. The first tourmaline to have crystallized from the melt is that in the line rock. The Li in the melt was probably isotopically heavier than in the tourmaline because ^7Li prefers the strong bonds in the melt over the octahedral coordination in tourmaline. At the point of fluid saturation of the dikes, melt and fluid phases separated and appear to have coexisted, causing the fractionation of Li isotopes between them. If the isotopic composition of Li in tourmaline in each of the zones reflects the relative fractionation of Li isotopes in the melt and fluid, then the isotopically heavier Li in the pegmatite zone tourmaline suggests that ^7Li was enriched in the melt. This fractionation suggests that the bonds involved in the melt are stronger than the bonds of hydrated Li in the fluid. There are no experimental data on the fractionation of Li isotopes between melts and fluids, but this inference is supported by isotopic compositions of Li in fluid inclusions and host quartz in the Tin Mountain pegmatite in the Black Hills (Teng *et al.*, 2006). Li in the fluid inclusions has much lower $\delta^7\text{Li}$ values than Li in the quartz, supporting Teng *et al.* (2006) that ^7Li prefers the stronger bonds in quartz where Li is possibly charge balancing Al incorporated into the quartz structure, and by analogy bonds in high-silica melts, over the weaker hydrated bonds in the fluid.

The $\delta^7\text{Li}$ values in tourmaline that crystallized in the pocket are similar to those in the line rock tourmaline. This is consistent with accumulation of the bulk of initial Li

that was in the original melt to the pocket fluid, as this would result in little change in the isotopic composition of the Li. Tourmaline in the two zones reflects the isotopic composition of the initial Li. Spodumene in the Tin Mountain pegmatite demonstrates similar behavior as its $\delta^7\text{Li}$ values are nearly the same across all zones of the pegmatite, which was attributed to the large concentration of Li incorporated into the spodumene where the compatibility of Li in the mineral overwhelms the ability of the isotopes to fractionate (Teng *et al.*, 2006).

Schorl crystals with elbaite rims collected from the pocket have different $\delta^7\text{Li}$ in the rims than the cores, with $\delta^7\text{Li}$ inversely correlated to Li concentration, Li in the black schorl cores is isotopically heavier than in the elbaite rims. This suggests that the schorl crystallized while melt was still present, which is also supported by its iron-rich composition as the Fe was sourced more likely from the melt than the fluid. The elbaite rims probably formed later in the presence of the fluid only, as suggested by the fact that it is a Li-bearing tourmaline and its $\delta^7\text{Li}$ value is smaller.

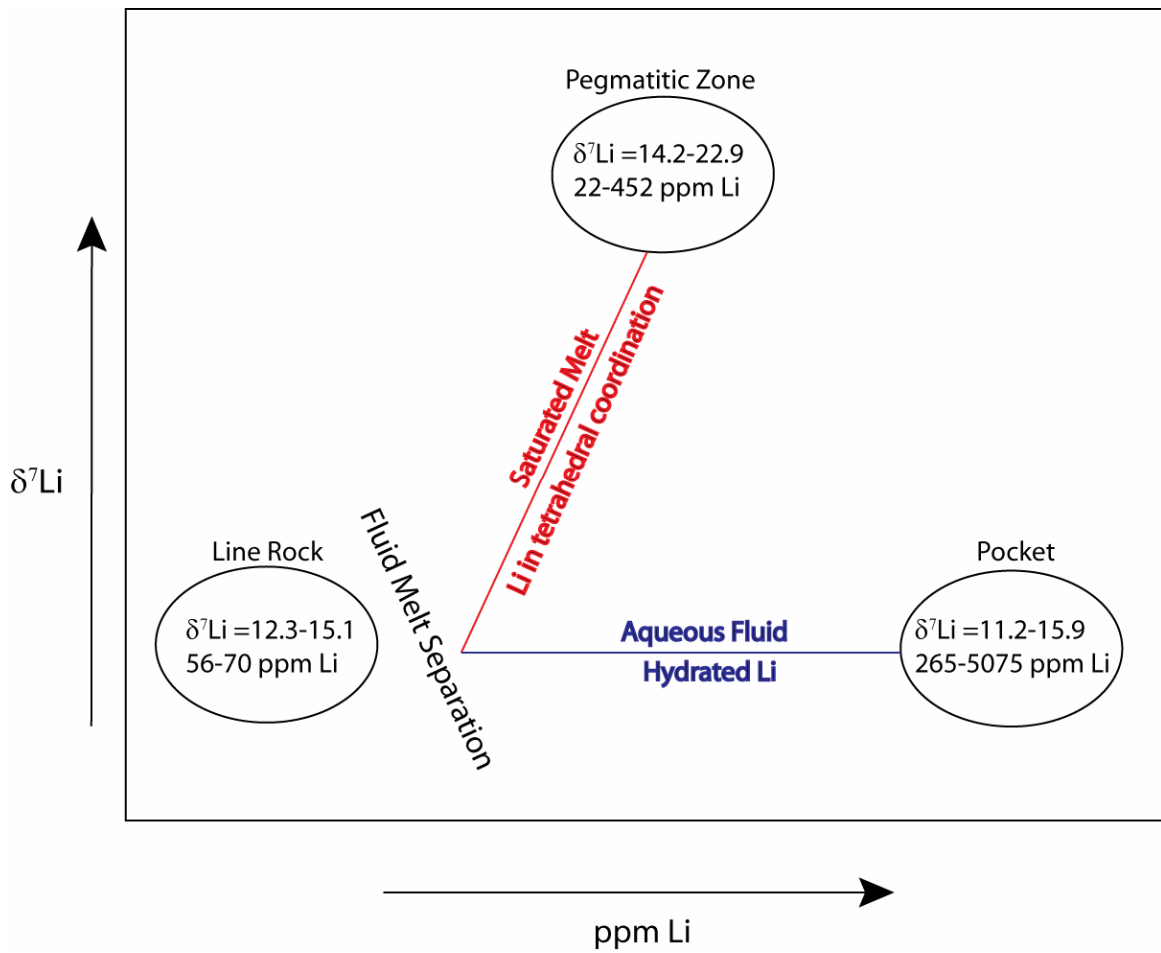


Figure 10: Schematic of Li and Li isotopic behavior in a pegmatitic melt.

Conclusions

Lithium concentration and isotopic ratio variances across zones of pegmatites can give insight into the processes that formed these interesting dikes. The pegmatites of San Diego County, California have similar structure, mineralogy, and geochemistry throughout all pegmatite districts. Tourmaline in the line rock has the lowest Li concentration, while tourmaline found in the pocket zone has the highest. Lithium behaved as an incompatible element and was enriched through progressive crystallization of the pegmatite. Crystallization of the line rock occurred first and continued until the melt reached fluid saturation. This point is marked by the increased grain size of the pegmatitic zone and Li concentration in tourmaline.

The initial concentration of Li of the melt is estimated to be ~1120 ppm, or ~0.5 mol % Li_2O , which is one to two orders of magnitude higher than that in the Harney Peak Granite in the Black Hills of South Dakota. The high concentration of fluxing components, Li and mostly H_2O , in the melt caused depolymerization of the melt that lowered its viscosity and increased diffusion rates, allowing for crystallization at temperatures $<400^\circ\text{C}$ without the dike solidifying to a glass.

The Li isotopic ratio of tourmaline is reflective of the medium from which it crystallized. ^7Li prefers stronger charge balancing sites in the melt while ^6Li fractionates into weaker octahedral sites in tourmaline and into the weak hydrated bonds in the fluid. As such, tourmaline in the line rock would have crystallized from a melt that was isotopically heavier. At the point of fluid saturation when melt and fluid separated, but appear to have coexisted, ^7Li was enriched in the melt suggesting that the hydrated bonds

in the fluid are weaker than the tetrahedral bonds in the melt. The $\delta^7\text{Li}$ values of tourmaline that crystallized in the pocket are similar to those found in the line rock as bulk of the initial Li from the original melt accumulated in the pocket fluid. The fractionation between melt and fluid can be seen in zoned tourmaline with isotopically heavy schorl cores that probably crystallized with melt still present and isotopically lighter elbaite rims that probably crystallized from fluid alone.

The behavior of Li and Li isotopes suggests that the San Diego County pegmatites crystallized by a process similar to that described by Jahns and Burnham (1969) and Walker *et al.* (1989). Crystallization started in the hanging wall and footwall and proceeded inward. Crystallization occurred as the melt evolved from fluid-unsaturated to fluid-saturated, while the pockets crystallized from the exsolved fluid that has gathered to form a bubble in the center of the dike. The gem and specimen quality elbaite tourmaline crystals in the pockets crystallized from fluid alone, in the absence of melt.

The crystallization of the pegmatite in a closed system is also supported by clay minerals found in the pocket from the dissolution of feldspars by the fluids, fracture fillings from the pocket outward which formed during rupture of the pocket and migration of the fluids through the fracture, and late-stage fluid alteration of albite and K-feldspar. If crystallization did not occur in a closed system, but rather through open-system fluid flow or metasomatism, there would be no progressive concentration of Li from the wall rock contact inward and no fractionation of the Li-isotopes, as there would not be coexisting phases for the isotopes to fractionate between.

Future studies of Li fractionation between other minor Li-bearing phases, such as lepidolite and spodumene, are warranted to further understand the behavior of Li during pegmatite crystallization.

References

- Bosi, F., Androozzi, G.B., Frederico, M., Graziani, G., Lucchesi, S. (2005). Crystal chemistry of the elbaite-schorl series. *American Mineralogist*. v.90. 1784-1792.
- Berhens, H., Meyer, M., Holtz, F., Benne, D., Nowak, M. (2001). The effect of alkali ionic radius, temperature, and pressure on the solubility of water in MAISi_3O_8 melts (M=Li, Na, K, Rb). *Chemical Geology*. v.174. 275-289.
- Brenan, J.M., Ryerson, F.J., Shaw, H.F. (1998). The role of aqueous fluids in the slab-to-mantle transfer to boron, beryllium, and lithium during subduction: Experiments and models. *Geochimica et Cosmochimica Acta*. v.62, 19-20. 3337-3347.
- Černý, P. (1991). Rare-element granitic pegmatites. Part I: Anatomy and internal evolution of pegmatite deposits. *Geoscience Canada*. V. 18, 2. 49-67.
- Clinkenbeard, J.P., and Walawender, M.J. (1989). Mineralogy of the La Posta pluton: Implications for the origin of zoned plutons in the eastern Peninsular Ranges batholith, southern and Baja California. *American Mineralogist*, v.74. 1258-1269.
- Deere, W.A., Howe, R.A., and Zussman, J. (1992). *An introduction to the rock-forming minerals*. 2nd Edition.
- Dingwell, D.B., Romano, C., Hess, K.U. (1996). The effect of water on the viscosity of a haplogranitic melt under P-T-X conditions relevant to silicic volcanism. *Contributions to Petrology and Mineralogy*. v.124. 19-28.
- Fisher, J. (2002). Gem and rare-element pegmatites of southern California. *Mineralogical Record*. v.33. 363-407.
- Fisher, J., Foord, E.E., Bricker, G.A. (1999). The geology, mineralogy, and history of the Himalaya Mine, Mesa Grande, San Diego County, California. *California Geology*. 3-17.
- Foord, E.E. (1976). Mineralogy and petrogenesis of layered pegmatite-aplite dikes in the Mesa Grande District, San Diego County, California. *Ph.D. Dissertation*. Stanford University.
- Gochenour, K. (2003). Diary of a discovery: Summer and fall 2001. *Rocks & Minerals*. v.78. 164-168.

- Gromet, L.P., and Silver, L.T. (1979). Profile of rare earth element characteristics across the Peninsular Ranges batholith near the international border, southern California, U.S.A., and Baja California, Mexico. In: P.L. Abbott and V.R. Todd Eds. *Mesozoic Crystalline Rocks: Peninsular Ranges batholith and pegmatites, Point Sal ophiolite*. 111-142.
- Hawthorne, F.C., and Henry D.J. (1999). Classification of the minerals in the tourmaline group. *European Journal of Mineralogy*. v.11. 201-215.
- Jahns, R.H., and Burnham, C.W. (1969). Experimental studies of pegmatite genesis: I. A model for the derivation and crystallization of granitic pegmatites. *Economic Geology*. v.64, 8. 843-864.
- Jahns, R.H., and Wright, L.A. (1951). Gem- and lithium-bearing pegmatites of the Pala District, San Diego County, California. *Special Report - California Division of Mines and Geology*. v. 1, 7-A. 1-72
- Jolliff, B.L., Papike, J.J., Shearer, C.K. (1986). Tourmaline as a recorder of pegmatite evolution: Bob Ingersoll Pegmatite, Black Hills, South Dakota. *American Mineralogist*. v. 71. 472-500.
- Kampf, A.R., Gochenour, K., Clanin, J. (2003). Tourmaline: Discovery at the Cryogenic Mine, San Diego County, California. *Rocks and Minerals*, v.78. 156-163.
- London, D., Hervig, R.L., Morgan, G.B. (1988). Melt-vapor solubilities and elemental partitioning in peraluminous granite-pegmatite systems: experimental results with Macusani glass at 200 MPa. *Contributions to Mineralogy and Petrology*., v.99. 360-373.
- Lynton, S.J., Walker, R.J., Candela, P.A. (2005). Lithium isotopes in the system Qz-Ms-fluid: An experimental study. *Geochimica et Cosmochimica Acta*. v.69, 13. 3337-3347.
- Morgan, G.B., and London, D. (1999). Crystallization of the Little Three layered pegmatite-aplite dike, Ramona District, California. *Contributions to Mineralogy and Petrology*, v.136. 310-330.
- Moriguiti, T., and Nakamura, E. (1998). High-yield lithium separation and the precise isotopic analysis for natural rock and aqueous samples. *Chemical Geology*. v.145, 1-2. 91-104.
- Mysen, B.O., and Richet, P. (2005). *Developments in Geochemistry 10: Silicate glasses and melts, properties and structure*. Elsevier.
- Perkins, D. (2002). *Mineralogy*. Prentice Hall.

- Qi, H.P., Taylor, P.D.P., Berglund, M., Be Bievre, P. (1997). Calibrated measurements of the isotopic composition and atomic weight of the natural Li isotopic reference material IRMM-016. *International Journal of Mass Spectrometry*. v.171, 1-3. 263-268.
- Romano, C., Poe, B., Mincione, V., Hess, K.U., Dinwell, D.B. (2001). The viscosities of dry and hydrous $XAlSi_3O_8$ ($X=Li, Na, K, Ca_{0.5}, Mg_{0.5}$) melts. *Chemical Geology*. v.174. 115-132.
- Rudnick, R.L., Tomascack, P.B., Njo, H.B., Gardner, L.R. (2004). Extreme lithium isotopic fractionation during continental weathering revealed in sapprolites from South Carolina. *Chemical Geology*, v. 212. 45-57.
- Silver, L.T., Taylor, H.P., Chappell, B. (1979). Some petrological, geochemical and geochronological observations of the Peninsular Ranges batholith near the international border of the U.S.A. and Mexico. In: P.L. Abbott and V.R. Todd Eds. *Mesozoic Crystalline Rocks: Peninsular Ranges batholith and pegmatites, Point Sal ophiolite*. 83-110.
- Sirbescu, M.-L., Nabelek, P.I. (2003). Crustal melts below 400°C. *Geology*. v.31, 8. 685-688.
- Sirbescu, M.-L. (2007) Personal Communications.
- Stern, L.A., Brown, G.E., Bird, D.K., Jahns, R.H., Foord, E.E., Shigley, J.E., Spaulding, L.B. (1986). Mineralogy and geochemical evolution of the Little Three pegmatite-aplite layered intrusive, Ramona, California. *American Mineralogist*, v.71. 406-427.
- Symons, D.T.A., Walawender, M.J., Smith, T.E., Molnar, S.E., Harris, M.J., Blackburn, W.H. (2003). Palomagnetism and geobarometry of the La Posta pluton, California. In: S.E. Johnson, S.R. Paterson, J.M. Fletcher, D.L. Kimbrough, A. Martin-Barajas Eds. *GSA Special Paper 374: Tectonic Evolution of Northwestern Mexico and the Southwestern USA*. 93-116.
- Taylor, M.C. (2005). Personal Communications.
- Taylor, B.E., Foord, E.E., Friedrichsen, H. (1979). Stable isotope and fluid inclusion studies of gem-bearing granitic pegmatite-aplite dikes, San Diego County, California. *Contributions to Mineralogy and Petrology*. v. 68. 187-205.
- Teng, F.-Z., McDonough, W.F., Rudnick, R.L., Dalpé, C., Tomascak, P.B., Chappell, B.W., Gao, S. (2004). Lithium isotopic composition and concentration of the

- upper continental crust. *Geochimica et Cosmochimica Acta*, v.68, n10. 4167-4178.
- Teng, F.-Z., McDonough, W.F., Rudnick, R.L., Walker, R.J., Sirbescu, M.-L. (2006). Lithium isotopic systematics of granites and pegmatites from the Black Hills, South Dakota. *American Mineralogist*, v. 91. 1488-1498.
- Walawender, M.J. (1979). Basic plutons of the Peninsular Ranges batholith, southern California. In: P.L. Abbott and V.R. Todd Eds. *Mesozoic Crystalline Rocks: Peninsular Ranges batholith and pegmatites, Point Sal ophiolite*. 151-162.
- Walawender, M.J., Gastil, R.G., Clinkenbeard, J.P., McCormick, W.V., Eastman, B.G., Wernicke, R.S., Wardlaw, M.S., Gunn, S.H., Smith, B.M. (1990). Origin and evolution of the zoned La Posta-type plutons, eastern Peninsular Ranges batholith, southern and Baja California. In: J.L. Anderson Ed. *GSA Memoir 174: The Nature and Origin of Cordilleran Magmatism*. 1-18.
- Walker, R.J., Hanson, G.N., Papike, J.J., O'Neil, J.R., and Laul, J.C. (1986). Internal Evolution of the Tin Mountain pegmatite, Black Hills, South Dakota. *American Mineralogist*. v. 71, 3-4. 440-459.
- Webber, K.L., Falster, A.U., Simmons, W.B., Foord, E.E. (1997). The role of diffusion-controlled oscillatory nucleation in the formation of line rock in pegmatite-aplite dikes. *Journal of Petrology*, v.38, n.12. 1777-1791.
- Webber, K.L., Simmons, W.B., Falster, A.U., Foord, E.E. (1999). Cooling rates and crystallization dynamics of shallow level pegmatite-aplite dikes, San Diego County, California. *American Mineralogist*, v.84. 708-717.
- Webster, J.D., Holloway, J.R., Hervig, R.L. (1989). Partitioning of Lithophile trace elements between H₂O and H₂O+CO₂ fluids and topaz rhyolite melt. *Economic Geology*. v.84. 116-134.
- Wetmore, P.H., Herzig, C., Alsleben, H., Sutherland, M., Schmidt, K.L., Schultz, P.W., Paterson, S.R. (2003). Mesozoic tectonic evolution of the Peninsular Ranges of southern and Baja, California. In: S.E. Johnson, S.R. Paterson, J.M. Fletcher, D.L. Kimbrough, A. Martin-Barajas Eds. *GSA Special Paper 374: Tectonic Evolution of Northwestern Mexico and the Southwestern USA*. 93-116.
- Whittington, A., Richet, P., Behrens, H., François, H., Scaillet, B. (2004). Experimental temperature-X(H₂O)-viscosity relationship for leucogranites and comparison with synthetic silicic liquids. *Transactions of the Royal Society of Edinburgh: Earth Sciences*. v.95. 59-71.

- Wilke, M., Nabelek, P.I., Glascock, M.D. (2002). B and Li in Proterozoic metapelites from the Black Hills, U.S.A.: Implications for the origin of leucogranitic magmas. *American Mineralogist*, v. 37. 491-500.
- Wunder, B., Meixner, A., Romer, R.L., Heinrich, W. (2006). T-dependent isotopic fractionation of lithium between clinopyroxene and high-pressure hydrous fluids. *Contributions to Mineralogy and Petrology*. v.151. 112-120.
- Wunder, B., Meixner, A., Romer, R.L., Feenstra, A., Schettler, G., Heinrich, W. (2007). Lithium isotope fractionation between Li-bearing staurolite, Li-mica and aqueous fluids: An experimental study. *Chemical Geology*. v. 238. 277-290.